HHS Public Access

Exosomal miR-9 released from HIV Tat stimulated astrocytes mediates microglial migration

Lu Yang[1,*], **Fang Niu**[2,*], **Honghong Yao**[3,4], **Ke Liao**[2], **Xufeng Chen**[5], **Yeonhee Kook**[2], **Rong Ma**[6], **Guoku Hu**[2], and **Shilpa Buch**[2]

[1]School of Medicine, University of Electronic Science and Technology of China, Chengdu 610054, China

[2]Department of Pharmacology and Experimental Neuroscience, University of Nebraska Medical Center, Omaha, NE, USA

[3]Department of Pharmacology, Medical School of Southeast University, Southeast University, Nanjing, China

[4]Institute of Life Sciences, Key Laboratory of Developmental Genes and Human Disease, Southeast University, Nanjing, China

[5]The first Affiliated Hospital of Nanjing Medical University, Nanjing 210029, China

[6]Department of Pharmacology, Tongji Medical College, Huazhong University of Science and Technology, Wuhan, Hubei, 430030, China

Abstract

Chronic neuroinflammation still remains a common underlying feature of HIV-infected patients on combined anti-retroviral therapy (cART). Previous studies have reported that despite near complete suppression of virus replication by cART, cytotoxic viral proteins such as HIV trans-activating regulatory protein (Tat) continue to persist in tissues such as the brain and the lymph nodes, thereby contributing, in part, to chronic glial activation observed in HIV-associated neurological disorders (HAND). Understanding how the glial cells cross talk to mediate neuropathology is thus of paramount importance. MicroRNAs (miR) also known as regulators of gene expression, have emerged as key paracrine signaling mediators that regulate disease pathogenesis and cellular crosstalk, through their transfer via the extracellular vesicles (EV). In the current study we have identified a novel function of miR-9, that of mediating microglial migration. We demonstrate that miR-9 released from Tat-stimulated astrocytes can be taken up by microglia resulting in their migratory phenotype. Exposure of human astrocytoma (A172) cells to HIV Tat resulted in induction and release of miR-9 in the EVs, which, was taken up by microglia, leading in turn, increased migration of the latter cells, a process that could be blocked by both an exosome inhibitor GW4869 or a specific target protector of miR-9. Furthermore, it was also demonstrated that EV miR-9 mediated inhibition of the expression of target PTEN, via its binding to the 3'UTR

CONFLICT OF INTEREST

seed sequence of the PTEN mRNA, was critical for microglial migration. To validate the role of miR-9 in this process, microglial cells were treated with EVs loaded with miR-9, which resulted in significant downregulation of PTEN expression with a concomitant increase in microglial migration. These findings were corroborated by transfecting microglia with a specific target protector of PTEN, that blocked miR-9-mediated downregulation of PTEN as well as microglial migration. *In vivo* studies wherein the miR-9 precursor-transduced microglia were transplanted into the striatum of mice, followed by assessing their migration in response to a stimulus administered distally, further validated the role of miR-9 in mediating microglial migration. Collectively, our findings provide evidence that glial crosstalk via miRs released from EVs play a vital role in mediating disease pathogenesis and could provide new avenues for development of novel therapeutic strategies aimed at dampening neuropathogenesis.

Keywords

HIV; CNS; Extracellular Vesicles; miR-9; PTEN

INTRODUCTION

Persistent neuroinflammation is a hallmark feature of HIV disease in the era of combined antiretroviral therapy. Activation of resident glial cells and their migration within the CNS contribute significantly to neuronal dysfunction/injury associated with various neurodegenerative diseases including HIV-associated neurological disorders (HAND) (McArthur et al., 2010; Cai et al., 2016; Ojha et al., 2017). Microglia manifest as ramified cells with highly branched, motile cell processes under normal homeostasis within the CNS (Prinz et al., 2017). While exposed to pathological stimuli, these cells undergo phenotypic changes, migrate toward the toxic stimuli and elicit inflammatory responses. Those cells are crucial for host defense, however, under certain conditions, they can also contribute to the progress of neuropathology (Prinz et al., 2017). During HIV infection, release of extracellular trans-activating regulatory protein (Tat) from infected cells serves as the focal site for microglial migration and activation (Langford and Masliah, 2001; Cai et al., 2016). Another distant glia cell type-astrocytes could be continuously activated by Tat protein and produce various pro-inflammatory factors, resulting in the loss of supportive function for the neurons as well as the increased infiltration of immune cells and mobility of microglia. Although the reciprocal interactions between microglia and astrocytes have been indicated to play important role for the development of neurodegenerative disease including HAND, an important challenge is to understand the inter-communication mechanisms at different stages of disease and the signaling pathways involved in their crosstalk during progress.

Exosomes are membrane-enriched extracellular vesicles (EVs) that have a proposed diameter of about 30–100 nm and that carry a specific cargo that is delivered to the donor cells (Hu et al., 2016; Ojha et al., 2017). These vesicles are released by numerous types of cells both during normal homeostasis as well as under pathological conditions (Alexander et al., 2017; Andras et al., 2017). In recent years, there has been an escalated interest in the study of these vesicles as conduits for the delivery of information between cells within the same or across disparate tissues. Exosomes play both biological and pathological roles in

intercellular communication via their signature cargo molecules, which includes signaling mediators, proteins and genetic material, such as microRNA (miRNA) (Hu et al., 2012a; Bellingham and Hill, 2017; Sempere et al., 2017; Tosar et al., 2017). MiRNAs are small, evolutionarily conserved noncoding RNAs that are derived from much larger primary transcripts. MiRNA dysregulation has been associated with many neurodegenerative processes including but not limited to virus infections. For example, previous studies have demonstrated that miR-146a is upregulated in human microglial cells during HIV infection, regulating the inflammatory response by targeting the CCL8 chemokine (Rom et al., 2010). Findings from our group have also demonstrated that miR-9 is upregulated in microglial cells following exposure to HIV protein Tat, leading in turn, to activation of these cells via distinct signaling pathways (Yao et al., 2014). In other reports it has also been shown that exosomal let-7 via its binding to TLR7 receptor in neurons and microglia, can elicit neuronal death (Lehmann et al., 2012). It has also been shown that exposure of astrocytes to both HIV Tat and opiates can lead to shuttling of EV miR-29b from the astrocytes to neurons, resulting in injury of the latter cells (Hu et al., 2012b). Exosome-mediated transfer of miRs across cells thus underlies regulation of pathogenesis of HAND, representing an evolving area of research.

Similar to HIV$^+$ subjects on antiretroviral therapy (ART), SIV-infected rhesus macaques on ART, also demonstrated increased glial activation, neuronal loss as well as dysregulation of various signature miRNAs (Yelamanchili et al., 2010; Chaudhuri et al., 2013; Yelamanchili et al., 2015; Chivero et al., 2017). Interestingly, in the previous miRNA array data obtained from the brains (basal ganglia) of SIV+ macaques, among the various dysregulated miRs, miR-9 was found to be highly upregulated compared with the uninfected controls. Since mir-9 has already been shown to activate microglia (Yao et al., 2014), in this study we sought to examine whether upregulated miR-9 released from Tat stimulated astrocytes could impact yet another function of microglia – that of migration.

PTEN (phosphatase and tensin homolog), is a negative regulator of Akt/PKB (protein kinase B) phosphorylation (Zhao et al., 2007). Dysregulation of PTEN gene and its related signaling has been implicated in various disease processes primarily via involvement of disruption of cell cycle, proliferation, apoptosis and cell mobility (Miyata et al., 2015; Yang et al., 2017). Several studies have also revealed the key role of PTEN in HIV-associated disease progression (Xue et al., 2014; Jensen et al., 2017; Sanchez-Del Cojo et al., 2017). For example, silencing the PTEN gene was protective against HIV Tat- induced neuronal death (Zhao et al., 2007). Another recent study revealed that the enhanced expression of miRs in Tat exposed cells was shown to be associated with the reduced expression of target PTEN thereby contributing to the disruption of cell cycle (Sanchez-Del Cojo et al., 2017).

In the current study, we demonstrate HIV Tat mediated induction and release of miR-9 in astrocyte EVs, which upon uptake by the microglia, resulted in enhanced migration of these latter cells. Additionally, our study also revealed PTEN as a target for miR-9 in microglia, with EV-miR-9-mediated PTEN pathway playing a role in the crosstalk between astrocytes and microglia and contributing, in turn, to microglial migration.

MATERIALS AND METHODS

Animal

C57BL/6N mice were purchased from Charles River Laboratories, Inc. (Wilmington, MA). CX3CR1-GFP mice were obtained from the Jackson Laboratory (Bar Harbor, Maine) and function by targeted deletion of CX3CR1 and GFP reporter insertion. All the animals were housed under conditions of constant temperature and humidity on a 12-h light, 12-h dark cycle, with lights on at 0700 h. Food and water were available *ad libitum*. Animals were deeply anesthetized by overdose of isoflurane followed by pneumothorax prior to perfusion. All animal procedures were performed according to the protocols approved by the Institutional Animal Care and Use Committee of the University of Nebraska Medical Center. HIV-, HIV+ patients' brain tissues were obtained from the National NeuroAIDS Tissue Consortium. Macaque brain tissues were collected from our previous study (Bokhari et al., 2011).

Cell Culture

BV-2-immortalized cell line was obtained from Dr. Sanjay Maggirwar (University of Rochester Medical Center, Rochester, NY, USA) and was grown and maintained in Dulbecco's modified Eagle's medium (DMEM, Invitrogen, Carlsbad, CA) with 10% heat-inactivated fetal bovine serum (FBS; Atlanta Biologicals, Flowery Branch, GA) and 100 units/mL of penicillin and 100 μg/mL of streptomycin (Life Technologies, Carlsbad, CA) at 37°C and 5% CO_2 and used up to 20 passages.

The human astrocytoma cell line A172 (ATCC® CRL1620™) was purchased from American Type Culture Collection and was cultured in DMEM containing 10% FBS, and 100 units/mL of penicillin and 100 μg/mL of streptomycin at 37°C and 5% CO_2 and used up to 25 passages.

Human primary astrocytes obtained from ScienCell Research Laboratories were cultured in astrocyte medium containing astrocyte growth supplement, 2% heat inactivated FBS and 10 U/ml penicillin-streptomycin and incubated at 37°C in a 5% CO2-humidified incubator. According to the manufacturer's instructions, human primary astrocytes were used under 10 passages. The purity of primary astrocytes was asseseed by staining with GFAP. Only cells with purity of greater than 95% were used in our studies.

Reagents

Recombinant Tat101 was purchased from ImmunoDiagnostics (Woburn, MA). Chemical inhibitors, including MβCD and DMA were purchased from Sigma (St. Louis, MO, USA). The miR-9 overexpression plasmid has-miR-9-1, miR-control, and miR-9 inhibitor plasmid hsa-miR-9-5p-locker/hsa-miR-9-3p-locker as well as miR-locker-control plasmids and lentiviruses were purchased from Biosettia (San Diego, CA).

Isolation of exosomes

EVs were isolated from the supernatant of A172 cells by differential centrifugation as previously described (Hu et al., 2012b; Hu et al., 2013). Briefly, conditioned media from

control, Tat101 or exosome release inhibitor (DMA and MβCD) exposed A172 cells were harvested, centrifuged at 1,000 g for 10 min to eliminate cells, and again spun at 10,000 g for 30 min, followed by filtration through 0.22 μm filter to remove cell debris. EVs were pelleted by ultracentrifugation (Beckman Ti70 rotor, Brea, CA, USA) at 100,000g for 70 min. EVs were assessed for their protein content using BCA Protein Assay Kit (Pierce, Rockford, IL, USA). TSG101, Alix and CD63 were detected by western blot as exosome markers. EVs were further quantified by the Nanoparticle Tracking Analysis (NTA) Nanosight (model NS300, Malvern Instruments Ltd, United Kingdom). EVs isolated from A172 cell culture were also used to load miR-9 using Exo-Fect exosome transfection reagent (System Biosciences, Palo Alto, CA) according to the manufacturer's instructions.

Electron microscopy

EV pellets were prepared for negative staining employing a slightly modified procedure. Using wide-bore tips, 3μl of EVs was gently placed on 200-mesh formvar-coated copper grids, allowed to adsorb for 4–5min, and processed for standard uranyl acetate staining. In the last step, the grid was washed with three changes of PBS and allowed to semi-dry at room temperature before observation in TEM (Hitachi H7500 TEM, Tokyo, Japan).

Plasmid and oligo transfection

A172 cells were transfected with 0.5μg pEF6.mCherry-TSG101 plasmid (Addgene, Plasmid #38318, Cambridge, MA) and BV-2 cells were transfected with 0.5μg pcDNA3-Flag PTEN (Addgene, Plasmid #78777, Cambridge, MA) / control plasmid or target protector by using the Lipofectamin™ 3000 reagent (Invitrogen, Carlsbad, CA) according to the manufacturer's protocol. The transfection efficiency of plasmid was determined 24 hours post-transfection by either fluorescent microscopy or western blot analysis, respectively. The custom-designed PTEN-Target Protector negative control (TP-ctrl: scramble sequence: CTCCACAGGAAGGTATTTCTAGTCT) and PTEN-Target Protector (TP-PTEN: TAGTTTCAACATATAATTTGGTTTC) were purchased from Integrated DNA Technologies. TP-PTEN oligo selectively protects PTEN from being targeted by miR-9, without affecting endogenous levels of miR-9 or its interaction with other mRNA targets. BV-2 cells were transfected with 20nmol/L of the TP-ctrl and TP-PTEN for 24 hours, followed by EV-Tat/EV-miR9 exposure for another 24 hours.

Lentivirus transduction

BV-2 cells or A172 cells were transduced with miR-Control, miR-9 lentivirus with multiplicity of infection (MOI) of 100, followed by gentle swirling and incubation for 3 days at 37°C. The transduction efficiency was determined by detecting red fluorescent protein-positive microglia at the 4th day post-transduction.

Luciferase activity assays

A 39 bp PTEN 3'UTR segment (sense 5' -TCGAGGCGGCCGCCAAAGTTGTATATTAAAC-CAAAGTTT-3' and antisense 3'-CCGCCGGCGGTTTCAACATATAATTTGGTTTCAAAGATC-5') containing the putative miR-9 target site was cloned into the *Xho*I and *Xba*I sites of the pmirGLO vector. For

pmirGLO-PTEN 3′UTR-miR-9-target-mutant segment (sense 5'-
TCGAGGCGGCCGCCAAAGTTGTATATTAATGGTTTCTTT-3' and antisense 3'-
CCGCCGGCGGTTTCAACATATAATTACCAAAGAAAGATC-5')), the miR-9 target site
(ACCAAAG) within the PTEN 3′UTR was changed to (TGGTTTC). Followed the
manufacturer's protocol (Promega), HEK293 cells were seeded in 24-well plates. The miR-9
or scramble miRNA-control were co-transfected with pmirGLO-PTEN-3′UTR-miR-9-target
or pmirGLO-PTEN-3′UTR-miR-9-target-mutant luciferase reporter vector by using
lipofectamine 3000 (Invitrogen). Two days post transfection, the luciferase activity was
assessed with the Dual-Luciferase Reporter Assay (Promega). Firefly luciferase activity was
normalized by renilla luciferase activity and expressed as a percentage of the control
(Triplicated independent experiment, performed in 3 wells each time).

Western blotting

Treated cells were lysed using the Mammalian Cell Lysis kit (Sigma-Aldrich, St. Louis,
MO, USA) and quantified using the micro BCA Protein Assay kit (Pierce, Rockford, IL,
USA). Equal amounts of the proteins were electrophoresed in a sodium dodecyl sulfate-
polyacrylamide gel (10–12%) under reducing conditions followed by transfer to PVDF
membranes. The blots were blocked with 5% non-fat dry milk in phosphate buffered saline.
The western blots were then probed with antibodies recognizing the PTEN, CD63 and
Tsg101 (1:1000, Abcam, Cambridge, United Kingdom), Alix (1:1000, Santa Cruz, Dallas,
Texas, USA) and β-actin (1:1000, Sigma-Aldrich, St. Louis, MO, USA). The secondary
antibodies were alkaline phosphatase conjugated to goat anti mouse/rabbit IgG (1:5000).
Signals were detected by chemiluminescence and imaged on the FluorChem E Imaging
System (ProteinSimple, San Jose, CA, USA); densitometry was performed utilizing Image J
software (NIH, Bethesda, MD).

Real-time PCR

For quantitative analysis of mRNA expression, comparative real-time PCR was performed
with the use of the Taqman® Universal PCR Master Mix (Applied Biosystems, Foster City,
CA). Specific primers and probes for mature miR-9 and snRNA RNU6B were obtained from
Applied Biosystems. All reactions were run in triplicate. The amount of miR-9 was obtained
by normalizing to snRNA RNU6B and relative to control as previously reported (Hu et al.,
2012b; Yao et al., 2014; Hu et al., 2017).

In situ hybridization and immunostaining

Macaque brain sections were deparaffinized and subject to antigen retrieval with PBS.
Sections were pre-hybridized in hybridization buffer (50% formamide, 10 mM Tris-HCl, pH
8.0, 200 μg/mL yeast tRNA, 1X Denhardt's solution, 600 mM NaCl, 0.25% SDS, 1 mM
EDTA, 100ug/ml salmonnsperm DNA) for 1h at 37°C in a humidified chamber. LNA
modified miR-9, labeled at both the 5′ and 3′ ends with digoxigenin (Exiqon, Hilden,
Germany), was diluted to final concentration of 2 pM in hybridization buffer, heated to 65°C
for 5 min, and separately hybridized to the sections at 37°C overnight. The slides were then
washed three times in 2XSSC and twice in 0.2XSSC at 42°C. They were then blocked with
1% BSA, 3% normal goat serum in 1XPBS for 1h at room temperature and incubated with
anti-digoxigenin conjugated with horseradish peroxidase (1:200, Roche Diagnostics GmbH,

Mannheim, Germany) and anti-GFAP(1:500, sigma, St. Louis, MO) antibodies overnight at 4°C. The slides were washed twice with 1XTBS and incubated with Alexa Fluor 488 goat anti-rabbit IgG (1:400, Invitrogen, Carlsbad, CA) antibody for 1h at room temperature. This was followed by 3 times 1X TBS washes and signal amplification using TSA Cy5 kit (PerkinElmer, Waltham, MA) according to the manufacturer's protocol. The slides were mounted in Prolong gold anti-fade reagent with DAPI (Invitrogen, Carlsbad, CA). Same procedures to detect miR-9 and GFAP expression levels were done in A172 cells. The specificity of the miR-9 signal in FISH experiments was confirmed by comparing with a scrambled control. Unlike the miR-9, the scramble probe showed no signal in astrocytes.

BV-2 cells cultured on coverslips were fixed with 4% formaldehyde in PBS for 20 min at room temperature (RT). The coverslips were washed three times with PBS, permeabilized with 0.3% Triton X-100 for 30 min, rewashed three times, and blocked in 10% goat serum in PBS for 2h at RT. Anti-Iba1 (1:1000, Wako, Richmond, VA) were used for immunostaining. The coverslips were washed with PBS and incubated with Alexa Fluor 488 conjugated anti-rabbit IgG (Life Technologies, Carlsbad, CA) for 2h at RT. After a final washing with PBS, the coverslips were mounted with the Prolong gold anti-fade reagent with DAPI and the fluorescent images were acquired at RT on a Zeiss Observer. A Z1 inverted microscope with a (63×, numerical aperture 0.3) oil-immersion objective was used; images were processed using AxioVs 40 Version 4.8.0.0 software (Carl Zeiss MicroImaging GmbH).

Microglial migration *in vitro*

Migration of microglia *in vitro* was determined using QCM™ 5μm Chemotaxis Assay 24-well-Colorimetric kit (Millipore, Burlington, MA) as described in the manufacturer's protocol. Briefly, BV-2 cells were collected and resuspended in serum-free DMEM with 0.5% BSA at 1×10^6/ml. Then 200μl cell suspension was added to the upper compartment of inserts and treated with EVs isolated from mock/pre-miR-9/anti-miR-9-5/anti-miR-9-3 transfected A172 cells with/without Tat101 exposure, 500μl of serum free DMEM was added to the lower chamber. The transwell plates were incubated for 18h at 37°C, followed by staining the cells with Cell Stain and removing the cells remaining in the insert. Quantification of microglial migration was assessed by processing images and measuring the extracted stain from migrated cells using a Synergy Mx fluorescence plate reader (BioTek Instruments, Winooski, VT).

MiR-9 increased microglial migration *in vivo*

a. LPS was microinjected into the striatum of C57BL/6 mice using the microinjection parameters (coordinates 0.62 mm before the bregma, 2.5mm lateral from the sagittal midline at a depth of 3.5 mm to skull surface). Two weeks following LPS injection, microglia transfected with miR-control or miR-9 were transplanted (at 0.5 μl/min) into another site of striatum at the following coordinates (coordinates 0.62 mm before the bregma, 1.0 mm lateral from the sagittal midline at a depth of 3.5mm to skull surface). Animals were perfused at day 5 following cell transplantation and fluorescent images were acquired at RT on a Zeiss Observer. A Z1 inverted microscope with a (10×, numerical aperture 0.3) objective was used; images were processed using AxioVs 40 Version 4.8.0.0

software (Carl Zeiss MicroImaging GmbH). Photographs were acquired using an AxioCam MRm digital camera.

b. Lentivirus-miR-control or Lentivirus-miR-9 (4 μl) was microinjected into the corpus callosum (coordinates: 2.6 mm before the bregma, 0.0 mm lateral from the sagittal midline at a depth of 1.5 mm to skull surface) of CX3CR1-GFP knock in mice using the hamilton syringe at a rate of 0.5 μl/min. Seven days following lentivirus injection to allow for expression of miRs, LPS (1 μg/μl, 4μl) was microinjected into a distant site in the hippocampus (coordinates 2.6 mm before the bregma, 1.5 mm lateral from the sagittal midline at a depth of 1.5 mm to skull surface). Animals were perfused 24 h later, brains harvested and tissue sections assessed by fluorescent microscopy. A Z1 inverted microscope with (10× & 40×, numerical aperture 0.3) objectives was used; images were processed using AxioVs 40 Version 4.8.0.0 software (Carl Zeiss MicroImaging GmbH). Photographs were acquired using an AxioCam MRm digital camera.

Statistical analysis

Statistical analysis was performed using one-way analysis of variance with a post hoc Student t-test. Results were judged statistically significant if $p < 0.05$ by analysis of variance.

RESULTS

Enhanced expression of miR-9 in the brains of SIV/HIV-infected subjects

In a previous study we reported a panel of dysregulated miRNAs, such as miR-29b, miR-138 and miR-9 in the brains of SIV-infected macaques (Hu et al., 2012b). Herein we first sought to validate these findings by qPCR using RNA isolated from basal ganglia (BG) and frontal cortices (FC) of SIV+ subjects. As shown in Figures 1A & 1B, there was upregulated expression of miR-9 in both the basal ganglia and FC of SIV+ macaques compared with the uninfected controls. Due to paucity of human basal ganglia tissue we validated expression level of miR-9 in human FC tissue. As shown in Figure 1C and similar to the findings observed in macaque basal ganglia, there was increased expression of miR-9 in the frontal cortices of HIV infected versus uninfected samples. Upregulation of miR-9 was also validated in the basal ganglia of SIV-infected macaques that had encephalitis (SIVE) using *in situ* hybridization (ISH). As shown in Figure 1D, miR-9 was primarily upregulated in the astrocytes in macaques with SIVE compared with untreated controls. The next step thus was to examine whether exposure of human A172 cells to HIV Tat (as a surrogate of HIV infection) could lead to upregulation of miR-9. As shown in Figure 1E, HIV Tat (100ng/ml) significantly upregulated the expression of miR-9 in astrocytes. Further validation of these findings was done by ISH using DIG labeled-miR-9 probe. As shown in Figure 1F, in the presence of HIV Tat, A172 cells demonstrated increased expression of miR-9, which co-localized with GFAP (astrocyte marker) positivity.

HIV Tat induced the release of miR-9 in astrocyte EVs

It has been widely recognized that astrocytes communicate with various cells of the CNS through the release and uptake of EVs (Pegtel et al., 2014; Basso and Bonetto, 2016). Having determined the effect of HIV Tat on upregulation of miR-9 in astrocytes, the next step was to examine the levels of miR-9 in EVs released from astrocytes stimulated with HIV Tat. To this end, we first isolated EVs from A172 human astrocyte conditioned media collected at 24h as described previously using differential ultracentrifugation (Hu et al., 2012b; Hu et al., 2013). EVs were characterized by transmission electron microscopy (TEM) and western blotting for exosomal markers. TEM image showed EVs of 40–100nm in diameter (Figure 2A). As shown in Figure 2B, immunoblotting of the EV lysates revealed the presence of the exosomal markers CD63, Alix and Tsg101. EVs isolated from conditioned media of A172 cells stimulated with HIV Tat (24h) or unstimulated were also validated by NanoSight Tracking Analysis (NTA). As shown in Figure 2C, Tat stimulated A172 cells demonstrated both increased numbers as well as size of EVs compared with EVs isolated from control A172 cells. Additionally, we also performed a time course of miR-9 expression in EVs release from Tat stimulated human primary astrocytes, and as shown in Figure 2D, there was elevated expression of miR-9 in EVs isolated from human primary astroyctes stimulated with HIV Tat for 24 h (~3.20 fold), followed by a drop in expression of miR-9 thereafter. Furthermore, these findings were also validated in A172 cells (Figure 2E). Additionally, in the A172 cells, we also found that pretreatment of cells with either the exosome inhibitor (dimethyl amiloride, DMA) or lipid-raft disrupting drug (methyl-β-cyclodex, MβCD), both of which are known to inhibit EV release abrogated HIV-Tat mediated upregualtion of miR-9 in isolated EVs (Figure 2E).

The next step was to examine the transfer of miR-9 from the astrocytes to the microglia. For this, A172 astrocytes were first transfected with either pEF6.mCherry-TSG101 (EV marker) or a control plasmid (pcDNA3.1) for 24 h, followed by isolation of EVs from the condition media. BV-2 microglia were then exposed to either control or experimental EVs (10 EVs/cell) for 1 h, and assessed for loclazition of mCherry-TSG101 in Iba 1 postive microglia. As observed in Figure 2F, microglia exposed to EVs from pEF6.mCherry-TSG101 plasmid transfected astrocytes, demonstrated a fine granular red fluorescence within the cytoplasm, suggesting thereby the incorporation of mCherry-TSG101 in the recipient BV-2 cells. Additionally, BV-2 cells exposed to EVs from Tat stimulated A172 astrocytes also demonstrated increased expression of miR-9 compared with BV-2 cells exposed to control EVs or BV-2 cells not exposed to EVs (Figure 2G).

MiR-9 from HIV Tat treated astrocytes promoted microglial migration via EVs

Both microglial activation as well as migration play critical roles in CNS pathogenesis including HAND. While it is known that miR-9 can impact microglial activation (Yao et al., 2014), whether miR-9 can also impact microglial migration remains unclear. We thus sought to examine if microglial uptake of EVs loaded with miR-9 could result in migration of microglia. BV-2 cells were cultured in the presence of EVs isolated from conditioned media harvested from A172 cells transduced with either pre-miR-9 or pre-control lentivirus and assessed for migration using Boyden Chambers. As shown in Figures 3A&3B, BV-2 cells cultured with EVs isolated from pre-miR-9 lentivirus transduced astrocytes demonstrated

increased migration compared with BV-2 cells cultured with EVs isolated from cells transduced with pre-control lentivirus. Since HIV Tat exposure of astrocytes resulted in increased expression and release of miR-9 in EVs, we next sought to examine the effect of EVs isolated from HIV Tat exposed astrocytes on microglial migration. Similar to the EVs isolated from miR-9 lentivirus transduced cells, there was significant increase in microglial mobility in presence of EVs isolated from HIV Tat stimulated astrocytes (Figures 3A&3B). To further confirm the specificity of EV miR-9 in mediating microglial migration, astrocytes were first transduced with anti-miR-9 lentivirus, to specifically block the expression of miR-9, followed by exposure of cells to HIV Tat protein. EVs were then isolated and exposed to microglia for assessment of microglial mobility. As shown in Figures 3C&3D, treatment of microglia with EVs isolated from A172 astrocytes transduced with anti-miR-9 lentivirus followed by exposure to Tat failed to enhance migration of BV-2 cells.

MiR-9-mediated regulation of microglial migration via targeting PTEN

Based on bioinformatics studies, PTEN has been shown to be a target of miR-9 (Figure 4A). Since PTEN gene with phosphatase activity is involved in various cellular processes such as proliferation, migration, cell-cycle regulation, we sought to examine whether astrocyte EV-miR-9 mediated regulation of microglial migration involved the target PTEN in recipient microglia. Having determined the uptake of EVs containing miR-9 by microglial cells, it was subsequently important to determine whether the transferred miR-9, once inside the cells, could bind directly to the 3′-untranslated region (3'UTR) of the target mRNA and inhibit its translation. To this end, HEK293 cells were transfected with a PTEN-3'UTR luciferase reporter construct, wherein luciferase expression was regulated by the PTEN 3'UTR, an miR-9 potential binding element (Figure 4A). Co-transfection of HEK293 cells with both miR-9 and PTEN-3'UTR-luciferase constructs resulted in a significant decrease in luciferase activity, suggesting thereby the preferential binding of miR-9 with the 3'UTR of PTEN. As a negative control, cells were also co-transfected with a construct containing mutations in the miR-9-binding region of the PTEN 3'UTR. As expected, in cells transfected with the PTEN 3'UTR mutant, miR-9 failed to downregulate luciferase activity (Figure 4C). Further confirmation of the role of miR-9 in regulating PTEN translation was carried out by overexpressing miR-9 in BV-2 cells, by transducing the cells with lentivirus-miR-9 and subsequently assessing the expression of PTEN protein by western blot. As shown in Figure 4D, cells transduced with lentivirus-miR-9 demonstrated reduced expression of endogenous PTEN protein compared with cells transduced with an unrelated control lentivirus. We next exposed BV-2 cells with EVs loaded with either control miRNA or miR-9 oligos, followed by monitoring expression of PTEN by western blot. As shown in Figure. 4E, similar to miR-9 lentivirus transduced cells, miR-9 loaded EVs also repressed the expression of PTEN compared to cells exposed to control EVs. Intriguingly, EVs isolated from HIV Tat stimulated A172 cells also demonstrated significant inhibition of PTEN levels in BV-2 cells compared with cells exposed to EVs isolated from control A172 cells (Figure 4F).

PTEN overexpression rescued EV-miR-9-induced microglial migration

To further confirm that PTEN was the key modulator in EV-miR-9-mediated microglial migration, BV-2 cells were transfected with either Flag-PTEN construct lacking the UTRs

(therefore not targeted by miR-9), or a control vector, followed by exposure to EVs isolated under various conditions. Expression of PTEN in FLAG-PTEN and control cells was assessed by western blotting. As shown in Figures 5A&5B, EVs isolated from conditioned media of HIV Tat stimulated A172 cells or EVs loaded with miR-9, failed to downregulate the expression of PTEN in Flag-PTEN expressing cells. In keeping with these findings, in BV-2 cells overexpressing Flag-PTEN, exposure to EVs from Tat stimulated A172 conditioned media or to EVs loaded with miR-9, failed to induce microglial migration (Figures 5C&5D).

PTEN as a functional target of miR-9

To further confirm whether the effect of miR-9 on PTEN was direct, BV-2 microglia were co-transfected with miR-9 oligos in the presence of either a target protector oligo (TP-PTEN) that specifically protected the miR-9 binding site on the endogenous PTEN 3'UTR or a scrambled target protector oligo (Figure 6A). As shown in Figures 6B & 6C, in the presence of a target protector oligo specific for miR-9 binding site, EVs isolated from either HIV Tat stimulated A172 conditioned media or those loaded with miR-9, failed to downregulate the expression of PTEN. Importantly, in BV-2 cells transfected with TP-PTEN, EVs isolated from HIV Tat stimulated A172 conditioned media or EVs loaded with miR-9 failed to induce microglial migration (Figures 6D&6E).

MiR-9 promotes microglial migration *in vivo*

In vivo validation of these findings was performed by transplanting miR-9 precursor/control miR-transduced microglia into the striatum of C57 wildtype mice followed by monitoring migration in response to LPS administered distally. As shown in Figures 7A & 7B, there was increased migration of miR-9-transduced microglia compared with miR-control transduced cells to the LPS-injected site. Further validation of these findings was carried out by microinjecting CX3CR1-GFP mice with either miR-control or miR-9 RFP-lentivirus (4 μl) in the corpus coliseum for 7 days, followed by injection of LPS (1μg/μl, 4μl) into the hippocampi of the same mice (Figure 7C). Twenty four hours later mice were sacrificed for assessment of migration of RFP miR-9 transduced/GFP microglia to the LPS injection site in hippocampal sections. As shown in Figures 7D&7E, there was significant increase of RFP miR-9-transduced/GFP microglia migrating to the LPS-injected site compared with the miR-control group.

DISCUSSION

HIV-1 has been described as a global health crisis despite the advent of ART (Maschke et al., 2000; Sacktor et al., 2002; Gray et al., 2003; McArthur et al., 2003). Microglial activation and migration are hallmark features of the innate inflammatory response within the CNS (Rivest, 2009). It is becoming increasingly appreciated that miR-mediated regulation of disease pathogenesis represents an evolving area of research that has ramifications for identification of potential therapeutic targets for various neurodegenerative disorders, for which currently there exists no cure. The highly conserved miR-9 plays critical roles in neurogenesis as well as in axonal extension (Radhakrishnan and Alwin Prem Anand, 2016). Its role in microglial migration, however, remains poorly understood. Herein

we identify a unique role of miR-9 in mediating microglial migration via EVs released from Tat-stimulated astrocytes. HIV Tat exposed astrocytes upregulate the expression & release of miR-9 in the EVs, that are taken up by the microglia, leading in turn, to increased microglial migration. MiR-9-mediated regulation of cellular migration involved downregulated expression of the target protein, PTEN that is a critical suppressor of cell motility. Furthermore, our *in vivo* data show that miR-9 promotes microglial migration in the brain.

Astrocytes, the most abundant type of cells in central nervous system (CNS), are crucial regulators of immune response during neuroinflammation. In addition to stimulation by HIV Tat (Chauhan et al., 2007; Bethel-Brown et al., 2011; El-Hage et al., 2011; Henderson et al., 2012; Fan and He, 2016; Hu et al., 2017), various other reports have also demonstrated activation of astrocytes by stimuli such as LPS (Tarassishin et al., 2014; Woodward et al., 2017), traumatic brain injury (TBI) (Burda et al., 2016) and psychostimulants such as cocaine/ methamphetamine (Shah et al., 2012; Zhang et al., 2015b; Zhang et al., 2015a; Periyasamy et al., 2016; Yu et al., 2017). Interestingly, LPS has also been shown to induce activation and expression of miR-9 in microglia (Yao et al., 2014). Whether LPS or other agents such as cocaine & TBI, can also induce miR-9 in astrocyte EVs, however, warrants further investigation.

EVs including exosomes have emerged as key regulators that function as 'bioactive vesicles' to promote cell-cell communication and immunoregulation. Kadiu *et al.* have demonstrated that the number of exosomes is significantly increased in HIV infected monocyte-derived macrophages (Kadiu et al., 2012). Furthermore, it was also shown that both HIV-1 infection and viral dissemination were accelerated by exosomes. In the CNS, EVs play an important role in mediating crosstalk among different cells, based on the premise that in the CNS many cells secrete these vesicles containing a specific cargo comprising of miRNAs, proteins, RNA and DNA, which can be transported to the recipient cells, and impair their functioning. Intriguingly, EVs released from HIV-infected cells contain HIV RNAs and HIV proteins, such as Tat, Gag and Nef, which in turn, following uptake by neighboring/distant cells also contribute to functional impairment of the receipt cells (Booth et al., 2006; Fang et al., 2007; Lenassi et al., 2010; Shelton et al., 2012; Narayanan et al., 2013; Jaworski et al., 2014; Rahimian and He, 2016; Raymond et al., 2016; Sampey et al., 2016). Elegant studies by Narayanan *et al.* have demonstrated that EVs released from HIV-1-infected cells contain HIV noncoding RNA (the trans-activation response element (TAR) (Narayanan et al., 2013). Intriguingly, uninfected cells cultured with TAR containing EVs are more susceptible to HIV-1 infection and confer a protective phenotype to these recipient cells under conditions of cellular stress (Narayanan et al., 2013). Similarly, EVs released from HIV infected cells can transport HIV proteins as well, such as Tat and Nef, to noninfected bystander cells leading to the release of proinflammatory cytokines and/or apoptosis (Lenassi et al., 2010; Rahimian and He, 2016; Sampey et al., 2016). Studies by Yelamanchili *et al.* have demonstrated that upregulated miR-21 in brain-derived EVs from SIV encephalitis causes neurotoxicity through the TLR7-dependent downstream necroptosis pathway (Yelamanchili et al., 2015). Recent studies have also highlighted the role of EV-mediated crosstalk between the CNS and the periphery. For example, novel studies by Dickens *et al.* have demonstrated that EVs released from interleukin-1β (IL-1β) stimulated astrocytes have the ability to rapidly cross the Blood-Brain Barrier (BBB) and enter the peripheral circulation, leading to

suppression of PPARα in the liver (Dickens et al., 2017). Recent exciting studies by Sun *et. al.* have also demonstrated that the number of neuron-derived EVs in plasma was significantly decreased in neuropsychologically impaired subjects compared with neuron-derived EVs from unimpaired subjects (Sun et al., 2017). Our previous studies have also demonstrated that SIV/SIV protein Tat and/or morphine altered the expression of astrocyte-released miR-29b, which, in turn, could be delivered via the exosomes to the neighboring neurons, resulting in targeted downregulation of the neurotrophic factor PDGF-B. In the current study we report that miR-9 can also be shuttled through EVs to regulate the migration of microglia in the brain, which further validates the role of EVs as a mediator between the CNS cells, in neurodegenerative diseases.

PTEN was originally identified as a multi-functional tumor suppressor (Li and Sun, 1997). Loss or mutation of PTEN has been observed in a large number of cancers, including prostate cancer, glioblastoma, endometrial, lung and breast cancer (Endersby and Baker, 2008). Mutation or depletion of PTEN leads to over-activation of Akt/PKB signaling pathway and, in turn, promotes cell mobility. Furthermore, in the CNS, PTEN can also activate extrasynaptic NMDA receptors (Ning et al., 2004), interact with p53 (Kurose et al., 2002), and dephosphorylate focal adhesion kinase (Tamura et al., 1999), thereby contributing to the neurotoxic effects of HIV-1 proteins, such as Tat and gp120 (Zhao et al., 2007; Zou et al., 2011). Interestingly, knockdown of PTEN by its siRNA showed protective effects on neurons against HIV Tat and gp120-induced neurotoxicity (Zhao et al., 2007; Zou et al., 2011). Additionally, Chugh *et al.* have demonstrated that HIV Tat significantly decreased PTEN levels in CHME5 (human fetal microglia cell line) cells (Chugh et al., 2007). Recent studies have also demonstrated that upregulation of PTEN in microglia significantly attenuated chronic constriction injury (CCI)-induced microglial activation and nociception in rat model of neuropathic pain. The role of PTEN in M1 (pro-inflammatory) or M2 (anti-inflammatory) microglial polarization has also been explored (Wang et al., 2015; Zhou et al., 2017). Herein, for the first time, we demonstrate that EV-miR-9-induced downregulation of PTEN expression enhanced microglial migration. Given the ability of EVs in spreading miRs and toxic proteins within the CNS, EV-miRNA-mediated microglial impairment could be envisioned as one of the many contributors mediating accelerated neurodegeneration in HAND.

In conclusion, our data suggest that exposure of astrocytes to HIV Tat induced the expression and secretion of miR-9 in the EVs, which, upon being taken up by the microglia, resulted in enhanced migration of these latter cells. EV-miR-9 is a positive regulator of microglial migration via its suppression of the target PTEN. These findings not only shed light on the mechanism(s) underlying the roles of EV-miRNAs on microglial dysfunction but also sets a stage for the future testing of EV-based therapeutic strategies using anti-miRNA or siRNA oligos for the treatment of HAND.

Acknowledgments

References

Alexander M, Ramstead AG, Bauer KM, Lee SH, Runtsch MC, Wallace J, Huffaker TB, Larsen DK, Tolmachova T, Seabra MC, Round JL, Ward DM, O'Connell RM. Rab27-Dependent Exosome Production Inhibits Chronic Inflammation and Enables Acute Responses to Inflammatory Stimuli. J Immunol. 2017

Andras IE, Leda A, Contreras MG, Bertrand L, Park M, Skowronska M, Toborek M. Extracellular vesicles of the blood-brain barrier: Role in the HIV-1 associated amyloid beta pathology. Mol Cell Neurosci. 2017; 79:12–22. [PubMed: 28040512]

Basso M, Bonetto V. Extracellular Vesicles and a Novel Form of Communication in the Brain. Front Neurosci. 2016; 10:127. [PubMed: 27065789]

Bellingham SA, Hill AF. Analysis of miRNA Signatures in Neurodegenerative Prion Disease. Methods Mol Biol. 2017; 1658:67–80. [PubMed: 28861783]

Bethel-Brown C, Yao H, Callen S, Lee YH, Dash PK, Kumar A, Buch S. HIV-1 Tat-mediated induction of platelet-derived growth factor in astrocytes: role of early growth response gene 1. J Immunol. 2011; 186:4119–4129. [PubMed: 21368226]

Bokhari SM, Hegde R, Callen S, Yao H, Adany I, Li Q, Li Z, Pinson D, Yeh HW, Cheney PD, Buch S. Morphine potentiates neuropathogenesis of SIV infection in rhesus macaques. J Neuroimmune Pharmacol. 2011; 6:626–639. [PubMed: 21431470]

Booth AM, Fang Y, Fallon JK, Yang JM, Hildreth JE, Gould SJ. Exosomes and HIV Gag bud from endosome-like domains of the T cell plasma membrane. J Cell Biol. 2006; 172:923–935. [PubMed: 16533950]

Burda JE, Bernstein AM, Sofroniew MV. Astrocyte roles in traumatic brain injury. Exp Neurol. 2016; 275(Pt 3):305–315. [PubMed: 25828533]

Cai Y, Yang L, Callen S, Buch S. Multiple Faceted Roles of Cocaine in Potentiation of HAND. Curr HIV Res. 2016; 14:412–416. [PubMed: 27009095]

Chaudhuri AD, Yelamanchili SV, Marcondes MC, Fox HS. Up-regulation of microRNA-142 in simian immunodeficiency virus encephalitis leads to repression of sirtuin1. FASEB J. 2013; 27:3720–3729. [PubMed: 23752207]

Chauhan A, Hahn S, Gartner S, Pardo CA, Netesan SK, McArthur J, Nath A. Molecular programming of endothelin-1 in HIV-infected brain: role of Tat in up-regulation of ET-1 and its inhibition by statins. FASEB J. 2007; 21:777–789. [PubMed: 17197385]

Chivero ET, Guo ML, Periyasamy P, Liao K, Callen SE, Buch S. HIV-1 Tat Primes and Activates Microglial NLRP3 Inflammasome-Mediated Neuroinflammation. J Neurosci. 2017; 37:3599–3609. [PubMed: 28270571]

Chugh P, Fan S, Planelles V, Maggirwar SB, Dewhurst S, Kim B. Infection of human immunodeficiency virus and intracellular viral Tat protein exert a pro-survival effect in a human microglial cell line. J Mol Biol. 2007; 366:67–81. [PubMed: 17157319]

Dickens AM, Tovar YRLB, Yoo SW, Trout AL, Bae M, Kanmogne M, Megra B, Williams DW, Witwer KW, Gacias M, Tabatadze N, Cole RN, Casaccia P, Berman JW, Anthony DC, Haughey NJ. Astrocyte-shed extracellular vesicles regulate the peripheral leukocyte response to inflammatory brain lesions. Sci Signal. 2017; 10

El-Hage N, Podhaizer EM, Sturgill J, Hauser KF. Toll-like receptor expression and activation in astroglia: differential regulation by HIV-1 Tat, gp120, and morphine. Immunol Invest. 2011; 40:498–522. [PubMed: 21425908]

Endersby R, Baker SJ. PTEN signaling in brain: neuropathology and tumorigenesis. Oncogene. 2008; 27:5416–5430. [PubMed: 18794877]

Fan Y, He JJ. HIV-1 Tat Induces Unfolded Protein Response and Endoplasmic Reticulum Stress in Astrocytes and Causes Neurotoxicity through Glial Fibrillary Acidic Protein (GFAP) Activation and Aggregation. J Biol Chem. 2016; 291:22819–22829. [PubMed: 27609520]

Fang Y, Wu N, Gan X, Yan W, Morrell JC, Gould SJ. Higher-order oligomerization targets plasma membrane proteins and HIV gag to exosomes. PLoS Biol. 2007; 5:e158. [PubMed: 17550307]

Gray F, Chretien F, Vallat-Decouvelaere AV, Scaravilli F. The changing pattern of HIV neuropathology in the HAART era. J Neuropathol Exp Neurol. 2003; 62:429–440. [PubMed: 12769183]

Henderson LJ, Sharma A, Monaco MC, Major EO, Al-Harthi L. Human immunodeficiency virus type 1 (HIV-1) transactivator of transcription through its intact core and cysteine-rich domains inhibits Wnt/beta-catenin signaling in astrocytes: relevance to HIV neuropathogenesis. J Neurosci. 2012; 32:16306–16313. [PubMed: 23152614]

Hu G, Drescher KM, Chen XM. Exosomal miRNAs: Biological Properties and Therapeutic Potential. Front Genet. 2012a; 3:56. [PubMed: 22529849]

Hu G, Liao K, Yang L, Pendyala G, Kook Y, Fox HS, Buch S. Tat-Mediated Induction of miRs-34a & -138 Promotes Astrocytic Activation via Downregulation of SIRT1: Implications for Aging in HAND. J Neuroimmune Pharmacol. 2017; 12:420–432. [PubMed: 28236278]

Hu G, Yang L, Cai Y, Niu F, Mezzacappa F, Callen S, Fox HS, Buch S. Emerging roles of extracellular vesicles in neurodegenerative disorders: focus on HIV-associated neurological complications. Cell Death Dis. 2016; 7:e2481. [PubMed: 27882942]

Hu G, Yao H, Chaudhuri AD, Duan M, Yelamanchili SV, Wen H, Cheney PD, Fox HS, Buch S. Exosome-mediated shuttling of microRNA-29 regulates HIV Tat and morphine-mediated neuronal dysfunction. Cell Death Dis. 2012b; 3:e381. [PubMed: 22932723]

Hu G, Gong AY, Roth AL, Huang BQ, Ward HD, Zhu G, Larusso NF, Hanson ND, Chen XM. Release of luminal exosomes contributes to TLR4-mediated epithelial antimicrobial defense. PLoS Pathog. 2013; 9:e1003261. [PubMed: 23592986]

Jaworski E, Saifuddin M, Sampey G, Shafagati N, Van Duyne R, Iordanskiy S, Kehn-Hall K, Liotta L, Petricoin E 3rd, Young M, Lepene B, Kashanchi F. The use of Nanotrap particles technology in capturing HIV-1 virions and viral proteins from infected cells. PLoS One. 2014; 9:e96778. [PubMed: 24820173]

Jensen K, Bikas A, Patel A, Kushchayeva Y, Costello J, McDaniel D, Burman K, Vasko V. Nelfinavir inhibits proliferation and induces DNA damage in thyroid cancer cells. Endocr Relat Cancer. 2017; 24:147–156. [PubMed: 28137980]

Kadiu I, Narayanasamy P, Dash PK, Zhang W, Gendelman HE. Biochemical and biologic characterization of exosomes and microvesicles as facilitators of HIV-1 infection in macrophages. Journal of immunology. 2012; 189:744–754.

Kurose K, Gilley K, Matsumoto S, Watson PH, Zhou XP, Eng C. Frequent somatic mutations in PTEN and TP53 are mutually exclusive in the stroma of breast carcinomas. Nat Genet. 2002; 32:355–357. [PubMed: 12379854]

Langford D, Masliah E. Crosstalk between components of the blood brain barrier and cells of the CNS in microglial activation in AIDS. Brain Pathol. 2001; 11:306–312. [PubMed: 11414473]

Lehmann SM, et al. An unconventional role for miRNA: let-7 activates Toll-like receptor 7 and causes neurodegeneration. Nat Neurosci. 2012; 15:827–835. [PubMed: 22610069]

Lenassi M, Cagney G, Liao M, Vaupotic T, Bartholomeeusen K, Cheng Y, Krogan NJ, Plemenitas A, Peterlin BM. HIV Nef is secreted in exosomes and triggers apoptosis in bystander CD4+ T cells. Traffic. 2010; 11:110–122. [PubMed: 19912576]

Li DM, Sun H. TEP1, encoded by a candidate tumor suppressor locus, is a novel protein tyrosine phosphatase regulated by transforming growth factor beta. Cancer Res. 1997; 57:2124–2129. [PubMed: 9187108]

Maschke M, Kastrup O, Esser S, Ross B, Hengge U, Hufnagel A. Incidence and prevalence of neurological disorders associated with HIV since the introduction of highly active antiretroviral therapy (HAART). J Neurol Neurosurg Psychiatry. 2000; 69:376–380. [PubMed: 10945813]

McArthur JC, Steiner J, Sacktor N, Nath A. Human immunodeficiency virus-associated neurocognitive disorders: Mind the gap. Ann Neurol. 2010; 67:699–714. [PubMed: 20517932]

McArthur JC, Haughey N, Gartner S, Conant K, Pardo C, Nath A, Sacktor N. Human immunodeficiency virus-associated dementia: an evolving disease. J Neurovirol. 2003; 9:205–221. [PubMed: 12707851]

Miyata S, Fukuda Y, Tojima H, Matsuzaki K, Kitanaka S, Sawada H. Mechanism of the inhibition of leukemia cell growth and induction of apoptosis through the activation of ATR and PTEN by the topoisomerase inhibitor 3EZ, 20Ac-ingenol. Leuk Res. 2015; 39:927–932. [PubMed: 26194899]

Narayanan A, Iordanskiy S, Das R, Van Duyne R, Santos S, Jaworski E, Guendel I, Sampey G, Dalby E, Iglesias-Ussel M, Popratiloff A, Hakami R, Kehn-Hall K, Young M, Subra C, Gilbert C, Bailey C, Romerio F, Kashanchi F. Exosomes derived from HIV-1-infected cells contain trans-activation response element RNA. J Biol Chem. 2013; 288:20014–20033. [PubMed: 23661700]

Ning K, Pei L, Liao M, Liu B, Zhang Y, Jiang W, Mielke JG, Li L, Chen Y, El-Hayek YH, Fehlings MG, Zhang X, Liu F, Eubanks J, Wan Q. Dual neuroprotective signaling mediated by downregulating two distinct phosphatase activities of PTEN. J Neurosci. 2004; 24:4052–4060. [PubMed: 15102920]

Ojha CR, Lapierre J, Rodriguez M, Dever SM, Zadeh MA, DeMarino C, Pleet ML, Kashanchi F, El-Hage N. Interplay between Autophagy, Exosomes and HIV-1 Associated Neurological Disorders: New Insights for Diagnosis and Therapeutic Applications. Viruses. 2017; 9

Pegtel DM, Peferoen L, Amor S. Extracellular vesicles as modulators of cell-to-cell communication in the healthy and diseased brain. Philos Trans R Soc Lond B Biol Sci. 2014; 369

Periyasamy P, Guo ML, Buch S. Cocaine induces astrocytosis through ER stress-mediated activation of autophagy. Autophagy. 2016; 12:1310–1329. [PubMed: 27337297]

Prinz M, Erny D, Hagemeyer N. Ontogeny and homeostasis of CNS myeloid cells. Nat Immunol. 2017; 18:385–392. [PubMed: 28323268]

Radhakrishnan B, Alwin Prem Anand A. Role of miRNA-9 in Brain Development. J Exp Neurosci. 2016; 10:101–120. [PubMed: 27721656]

Rahimian P, He JJ. Exosome-associated release, uptake, and neurotoxicity of HIV-1 Tat protein. J Neurovirol. 2016; 22:774–788. [PubMed: 27173397]

Raymond AD, Diaz P, Chevelon S, Agudelo M, Yndart-Arias A, Ding H, Kaushik A, Jayant RD, Nikkhah-Moshaie R, Roy U, Pilakka-Kanthikeel S, Nair MP. Microglia-derived HIV Nef+ exosome impairment of the blood-brain barrier is treatable by nanomedicine-based delivery of Nef peptides. J Neurovirol. 2016; 22:129–139. [PubMed: 26631079]

Rivest S. Regulation of innate immune responses in the brain. Nat Rev Immunol. 2009; 9:429–439. [PubMed: 19461673]

Rom S, Rom I, Passiatore G, Pacifici M, Radhakrishnan S, Del Valle L, Pina-Oviedo S, Khalili K, Eletto D, Peruzzi F. CCL8/MCP-2 is a target for mir-146a in HIV-1-infected human microglial cells. FASEB J. 2010; 24:2292–2300. [PubMed: 20181935]

Sacktor N, McDermott MP, Marder K, Schifitto G, Selnes OA, McArthur JC, Stern Y, Albert S, Palumbo D, Kieburtz K, De Marcaida JA, Cohen B, Epstein L. HIV-associated cognitive impairment before and after the advent of combination therapy. J Neurovirol. 2002; 8:136–142. [PubMed: 11935465]

Sampey GC, Saifuddin M, Schwab A, Barclay R, Punya S, Chung MC, Hakami RM, Zadeh MA, Lepene B, Klase ZA, El-Hage N, Young M, Iordanskiy S, Kashanchi F. Exosomes from HIV-1-infected Cells Stimulate Production of Pro-inflammatory Cytokines through Trans-activating Response (TAR) RNA. J Biol Chem. 2016; 291:1251–1266. [PubMed: 26553869]

Sanchez-Del Cojo M, Lopez-Huertas MR, Diez-Fuertes F, Rodriguez-Mora S, Bermejo M, Lopez-Campos G, Mateos E, Jimenez-Tormo L, Gomez-Esquer F, Diaz-Gil G, Alcami J, Coiras M. Changes in the cellular microRNA profile by the intracellular expression of HIV-1 Tat regulator: A potential mechanism for resistance to apoptosis and impaired proliferation in HIV-1 infected CD4+ T cells. PLoS One. 2017; 12:e0185677. [PubMed: 28968466]

Sempere LF, Keto J, Fabbri M. Exosomal MicroRNAs in Breast Cancer towards Diagnostic and Therapeutic Applications. Cancers (Basel). 2017; 9

Shah A, Silverstein PS, Singh DP, Kumar A. Involvement of metabotropic glutamate receptor 5, AKT/PI3K signaling and NF-kappaB pathway in methamphetamine-mediated increase in IL-6 and IL-8 expression in astrocytes. J Neuroinflammation. 2012; 9:52. [PubMed: 22420994]

Shelton MN, Huang MB, Ali SA, Powell MD, Bond VC. Secretion modification region-derived peptide disrupts HIV-1 Nef's interaction with mortalin and blocks virus and Nef exosome release. J Virol. 2012; 86:406–419. [PubMed: 22013042]

Sun B, Dalvi P, Abadjian L, Tang N, Pulliam L. Blood neuron-derived exosomes as biomarkers of cognitive impairment in HIV. AIDS. 2017

Tamura M, Gu J, Danen EH, Takino T, Miyamoto S, Yamada KM. PTEN interactions with focal adhesion kinase and suppression of the extracellular matrix-dependent phosphatidylinositol 3-kinase/Akt cell survival pathway. J Biol Chem. 1999; 274:20693–20703. [PubMed: 10400703]

Tarassishin L, Suh HS, Lee SC. LPS and IL-1 differentially activate mouse and human astrocytes: role of CD14. Glia. 2014; 62:999–1013. [PubMed: 24659539]

Tosar JP, Cayota A, Eitan E, Halushka MK, Witwer KW. Ribonucleic artefacts: are some extracellular RNA discoveries driven by cell culture medium components? J Extracell Vesicles. 2017; 6:1272832. [PubMed: 28326168]

Wang G, Shi Y, Jiang X, Leak RK, Hu X, Wu Y, Pu H, Li WW, Tang B, Wang Y, Gao Y, Zheng P, Bennett MV, Chen J. HDAC inhibition prevents white matter injury by modulating microglia/macrophage polarization through the GSK3beta/PTEN/Akt axis. Proc Natl Acad Sci U S A. 2015; 112:2853–2858. [PubMed: 25691750]

Woodward NC, Levine MC, Haghani A, Shirmohammadi F, Saffari A, Sioutas C, Morgan TE, Finch CE. Toll-like receptor 4 in glial inflammatory responses to air pollution in vitro and in vivo. J Neuroinflammation. 2017; 14:84. [PubMed: 28410596]

Xue M, Yao S, Hu M, Li W, Hao T, Zhou F, Zhu X, Lu H, Qin D, Yan Q, Zhu J, Gao SJ, Lu C. HIV-1 Nef and KSHV oncogene K1 synergistically promote angiogenesis by inducing cellular miR-718 to regulate the PTEN/AKT/mTOR signaling pathway. Nucleic Acids Res. 2014; 42:9862–9879. [PubMed: 25104021]

Yang N, Chen J, Zhang H, Wang X, Yao H, Peng Y, Zhang W. LncRNA OIP5-AS1 loss-induced microRNA-410 accumulation regulates cell proliferation and apoptosis by targeting KLF10 via activating PTEN/PI3K/AKT pathway in multiple myeloma. Cell Death Dis. 2017; 8:e2975. [PubMed: 28796257]

Yao H, Ma R, Yang L, Hu G, Chen X, Duan M, Kook Y, Niu F, Liao K, Fu M, Hu G, Kolattukudy P, Buch S. MiR-9 promotes microglial activation by targeting MCPIP1. Nat Commun. 2014; 5:4386. [PubMed: 25019481]

Yelamanchili SV, Chaudhuri AD, Chen LN, Xiong H, Fox HS. MicroRNA-21 dysregulates the expression of MEF2C in neurons in monkey and human SIV/HIV neurological disease. Cell Death Dis. 2010; 1:e77. [PubMed: 21170291]

Yelamanchili SV, Lamberty BG, Rennard DA, Morsey BM, Hochfelder CG, Meays BM, Levy E, Fox HS. MiR-21 in Extracellular Vesicles Leads to Neurotoxicity via TLR7 Signaling in SIV Neurological Disease. PLoS Pathog. 2015; 11:e1005032. [PubMed: 26154133]

Yu C, Narasipura SD, Richards MH, Hu XT, Yamamoto B, Al-Harthi L. HIV and drug abuse mediate astrocyte senescence in a beta-catenin-dependent manner leading to neuronal toxicity. Aging Cell. 2017; 16:956–965. [PubMed: 28612507]

Zhang Y, Zhu T, Zhang X, Chao J, Hu G, Yao H. Role of high-mobility group box 1 in methamphetamine-induced activation and migration of astrocytes. J Neuroinflammation. 2015a; 12:156. [PubMed: 26337661]

Zhang Y, Lv X, Bai Y, Zhu X, Wu X, Chao J, Duan M, Buch S, Chen L, Yao H. Involvement of sigma-1 receptor in astrocyte activation induced by methamphetamine via up-regulation of its own expression. J Neuroinflammation. 2015b; 12:29. [PubMed: 25889537]

Zhao T, Adams MH, Zou SP, El-Hage N, Hauser KF, Knapp PE. Silencing the PTEN gene is protective against neuronal death induced by human immunodeficiency virus type 1 Tat. J Neurovirol. 2007; 13:97–106. [PubMed: 17505978]

Zhou K, Zhong Q, Wang YC, Xiong XY, Meng ZY, Zhao T, Zhu WY, Liao MF, Wu LR, Yang YR, Liu J, Duan CM, Li J, Gong QW, Liu L, Yang MH, Xiong A, Wang J, Yang QW. Regulatory T cells ameliorate intracerebral hemorrhage-induced inflammatory injury by modulating microglia/macrophage polarization through the IL-10/GSK3beta/PTEN axis. J Cereb Blood Flow Metab. 2017; 37:967–979. [PubMed: 27174997]

Zou S, El-Hage N, Podhaizer EM, Knapp PE, Hauser KF. PTEN gene silencing prevents HIV-1 gp120(IIIB)-induced degeneration of striatal neurons. J Neurovirol. 2011; 17:41–49. [PubMed: 21234828]
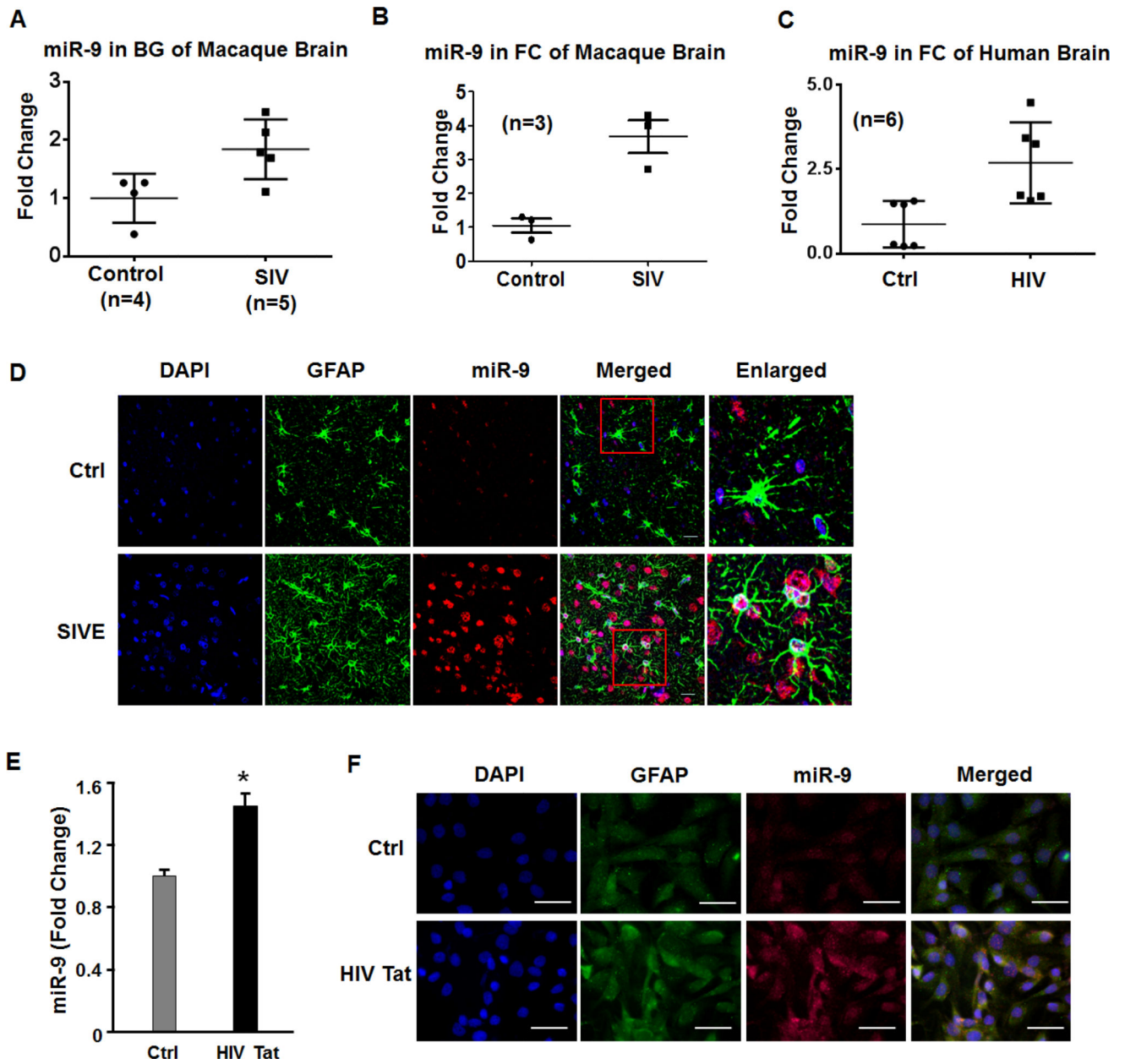
Figure 1. miR-9 is upregulated in HIV Tat stimulated astrocytes

(A, B) miR-9 expression in (A) the basal ganglia and (B) frontal cortex of SIV infected subjects. (C) miR-9 expression in the frontal cortex of HIV infected subjects. (D) Upregulation of miR-9 in the basal ganglia of SIV-infected macaques with encephalitis (SIVE) using *in situ* hybridization (ISH), in the astrocytes (GFAP+), scale bar=10 μm. (E) Real-time PCR analysis of miR-9 expression in A172 astrocytes treated with HIV Tat. (F) ISH demonstrating increased miR-9 in A172 astrocytes, scale bar=20 μm. Bars represent mean ± SD from 3 independent experiments. *p<0.05 vs control.
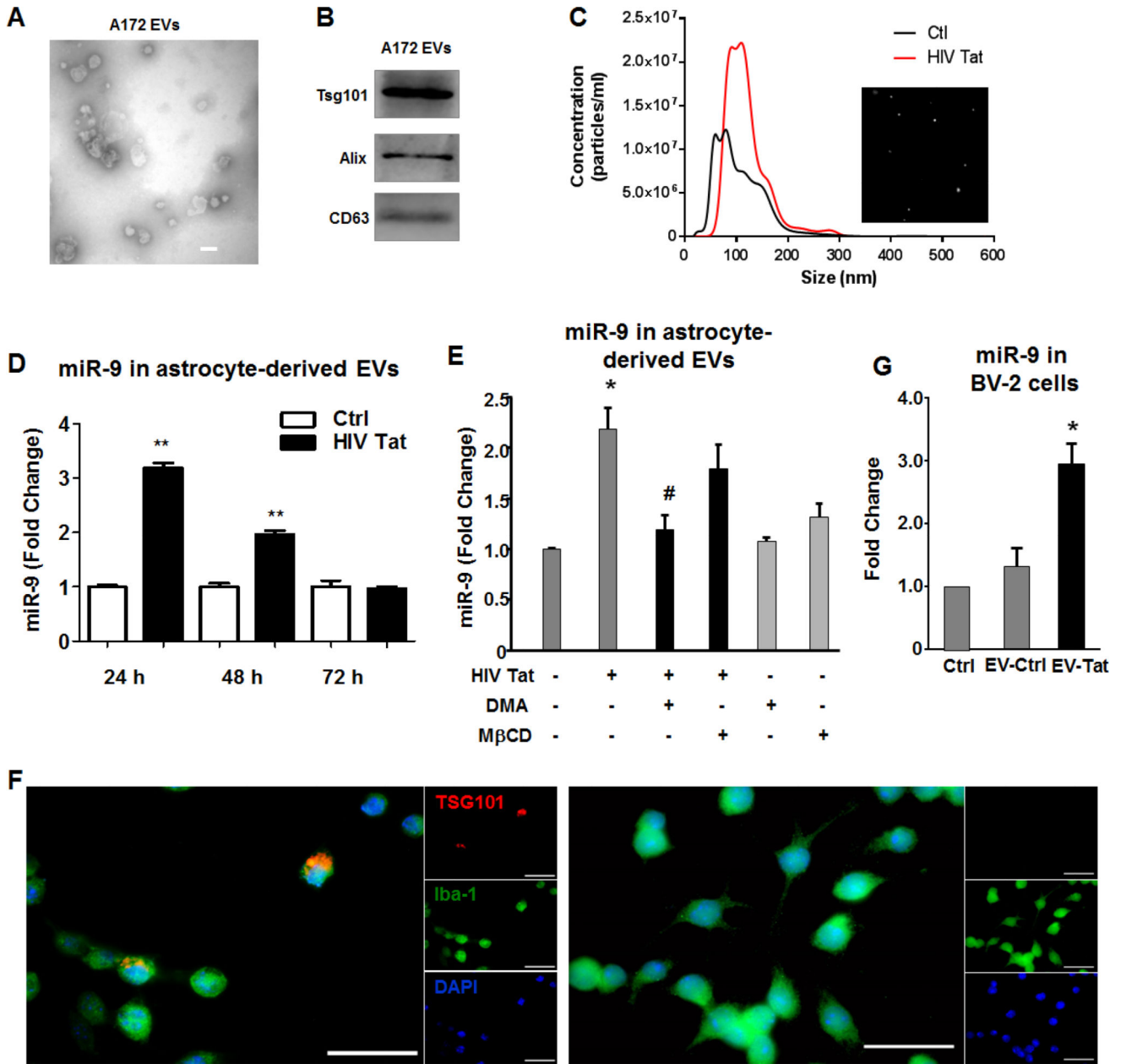
Figure 2. HIV Tat upregulates miR-9 in EVs released from astrocytes
EVs isolated from A172 astrocyte cultures were characterized by Transmission Electron microscopy (**A**). Scale bar 100 nm. (**B**) Western blot characterization of astrocyte EVs with exosome marker antibody against Tsg101, Alix, and CD63. (**C**) Size and particle distribution plots of isolated EVs from control A172 cells or A172 cells exposed to HIV Tat by NanoSight Tracking Analysis (NTA). The image shows increased size and number of vesicles released from A172 cells exposed to HIV Tat. (**D**) The time course of miR9 expresion in EVs released from human primary astrocytes exposed to HIV tat for 24 h, 48 h and 72 h. (**E**) A172 cells were pre-treated with exosome release inhibitor (DMA and MβCD) for 1 h, followed by Tat exposure for 24 h. Total RNA from EVs was analyzed by real-time PCR for miR-9. (**F**) Uptaken of EVs-TSG101-mcherry from A172 cells transfected with

either pEF6.mCherry-TSG101 (left) or pcDNA3.1 (right) plasmid by BV-2 cells; TSG101 (Exosome marker, red), Iba-1 (microglia marker, green), DAPI (nucleus, blue). Scale bar = 20 μm. **(G)** BV-2 cells exposed to EVs derived from Tat stimulated A172 cells showed increased miR-9 compared with BV-2 cells exposed to control EVs or BV-2 cells not exposed to EVs. Data are presented as mean ± SD of four individual experiments. * P < 0.05 compared with control. # P < 0.05 compared with Tat treatment.
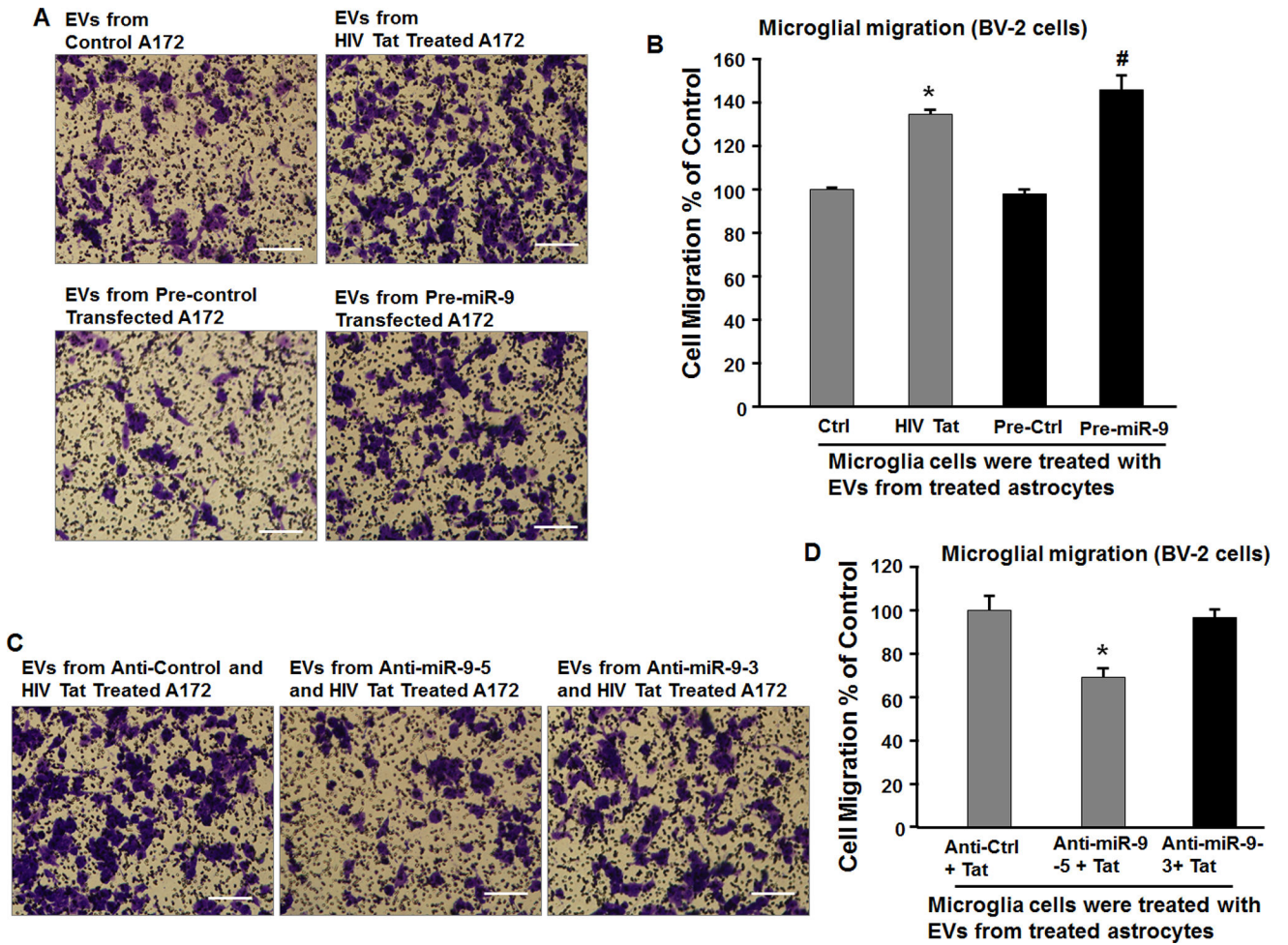
Figure 3. Increased migration of microglia treated with EVs released from Tat treated astrocyte cultures

(A, C) The representative phase images of migratory BV-2 stained by crystal violet. Scale bar = 5 μm. (B) EVs isolated from Tat or pre-miR-9 treated A172 cells treatments significantly increased the number of BV-2 cells that were capable of migrating through the membrane of the inserts. * $P < 0.05$ *versus* control; # $P < 0.05$ *versus* Pre-Ctrl. (D) EVs isolated from Tat and anti-miR-9 treated A172 cells treatments significantly decreased Tat-induced migratory BV-2 cells. * $P < 0.05$ *versus* Anti-Ctrl.
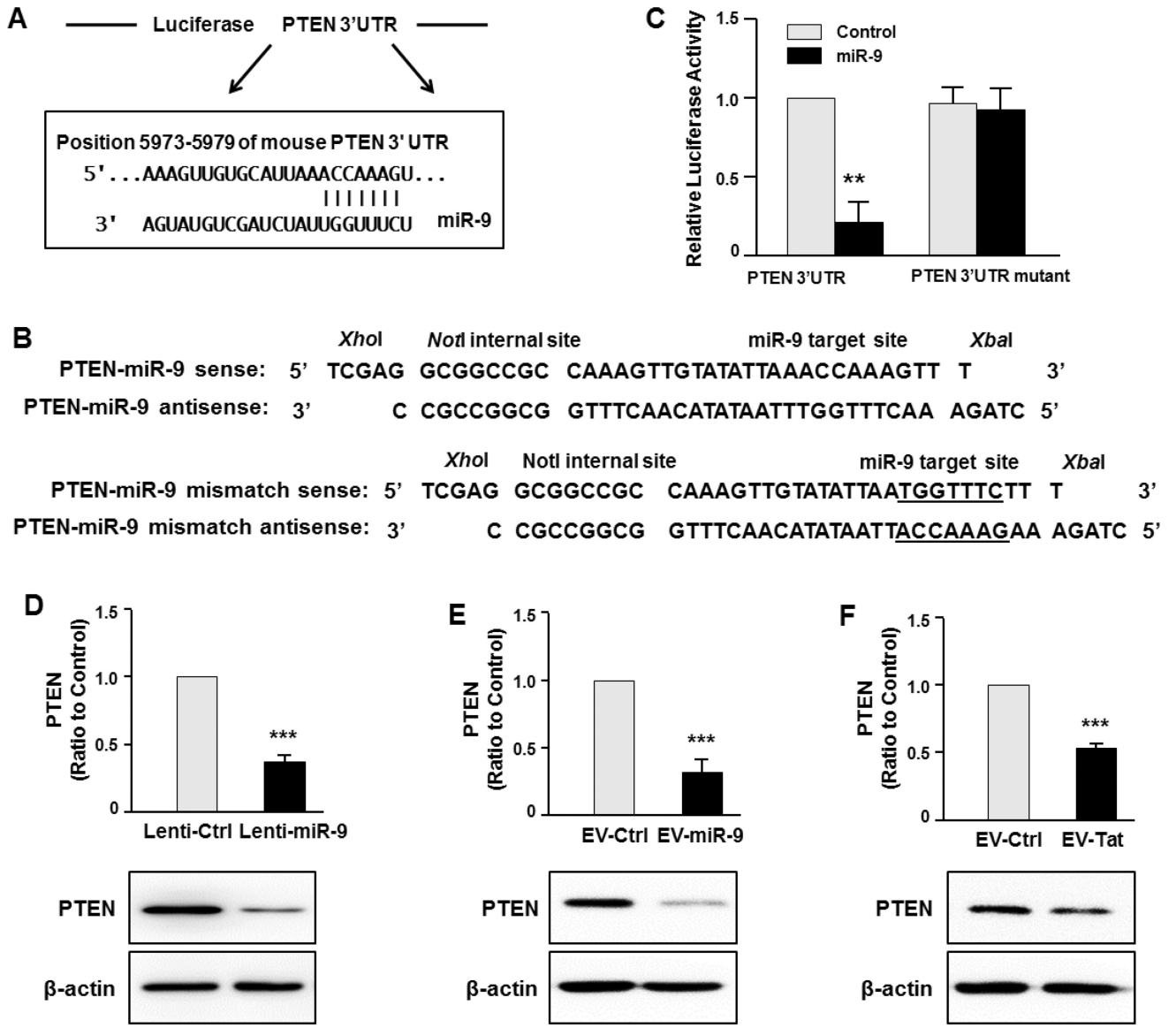
Figure 4. EV-miR-9 targets PTEN

(**A**) Putative miR-9 binding site in PTEN mRNA. (**B**) Cloning strategy of the PTEN 3′-UTR and mutant 3′-UTR downstream of the Luciferase reporter gene ORF vector. (**C**) Relative luciferase activity of WT/3′UTR mutant constructs of PTEN co-transfected with miR-control/miR-9. (**D–F**) Western blot analysis of PTEN protein levels in BV-2 cells transducted with control or miR-9 lentivirus (**D**), treated with EVs isolated from astrocytes loaded with control or miR-9 oligo (**E**), or treated with EVs isolated from control or HIV Tat exposed astrocytes (**F**).
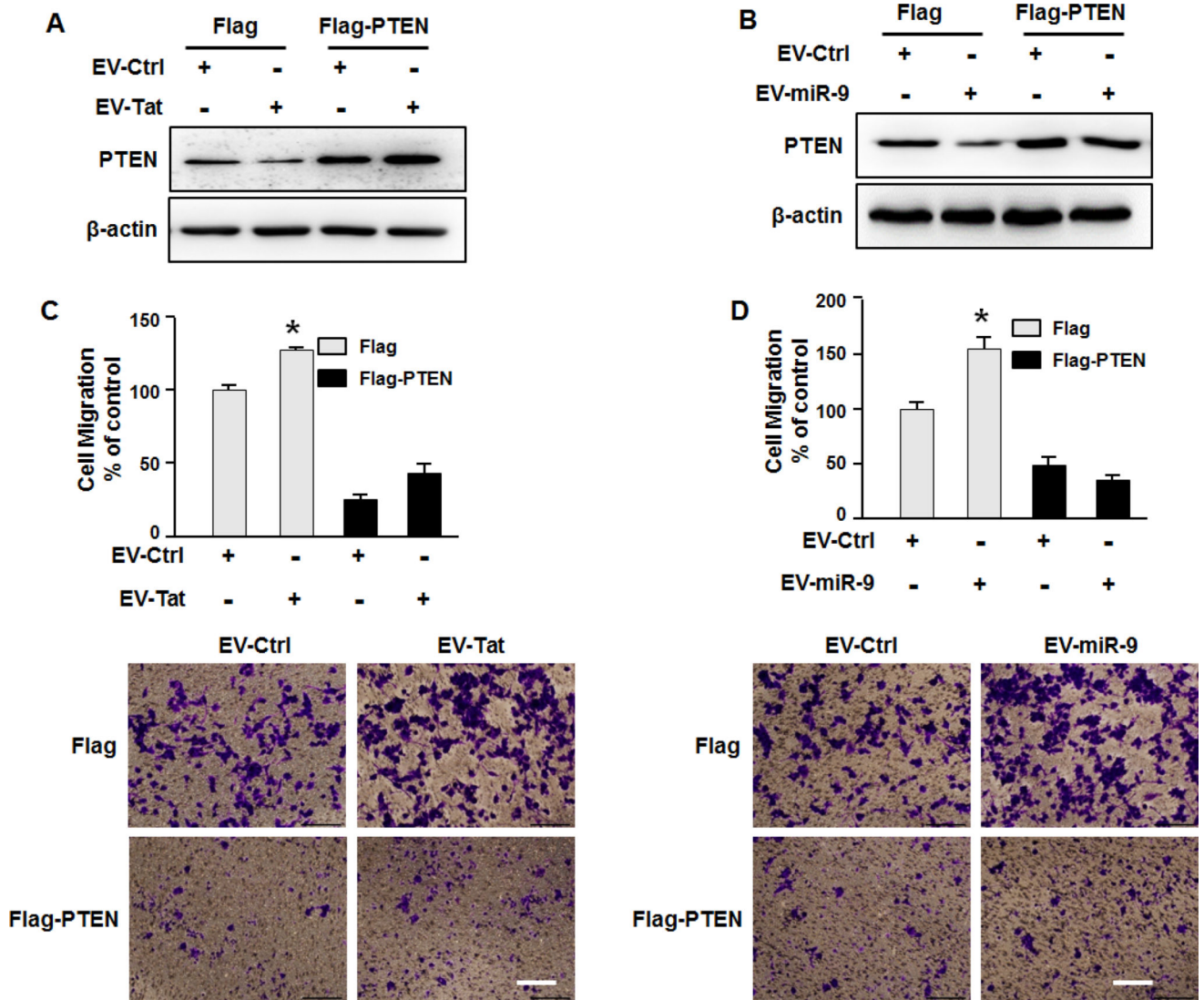
Figure 5. EV-miR-9-mediated microglial migration involves suppression of PTEN
(A, B) Transfection of BV-2 microglia with PTEN 3′UTR construct resulted in inhibition of EV isolated from Tat treated astrocytes and miR-9 loaded EV-mediated downregulation of PTEN. **(C, D)** EVs isolated from Tat treated astrocytes and miR-9-loaded-EVs failed to induce microglial migration in PTEN overexpressing cells. Scale bar = 5 μm. All the data are indicated as mean ± SD of 4 independent experiments. * $P < 0.05$.
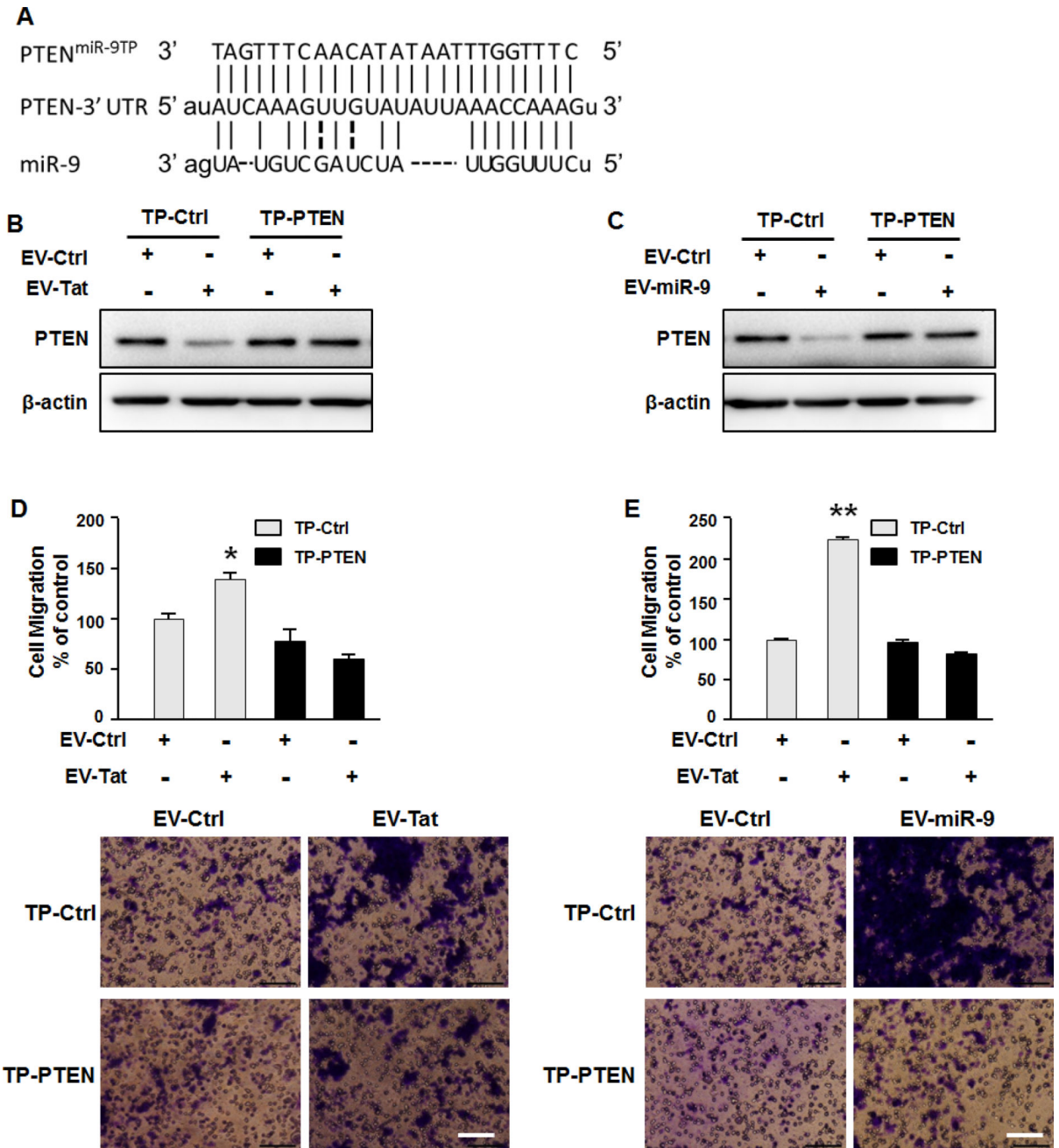
Figure 6. miR-9 in EVs induces microglial migration via binding PTEN 3'UTR

(A) Putative miR-9 and PTEN^miR-9TP binding sites in PTEN 3'UTR. (B, C) Transfection of BV-2 microglia with TP-PTEN oligo resulted in inhibition of EV isolated from Tat treated astrocytes and miR-9 loaded EV-mediated downregulation of PTEN. (D, E) EVs isolated from Tat treated astrocytes and miR-9-loaded-EVs failed to induce microglial migration in the presence of PTEN^miR-9TP oligo. Scale bar = 5 μm. All the data are indicated as mean ± SD of 4 independent experiments. *P<0.05, **P<0.01.
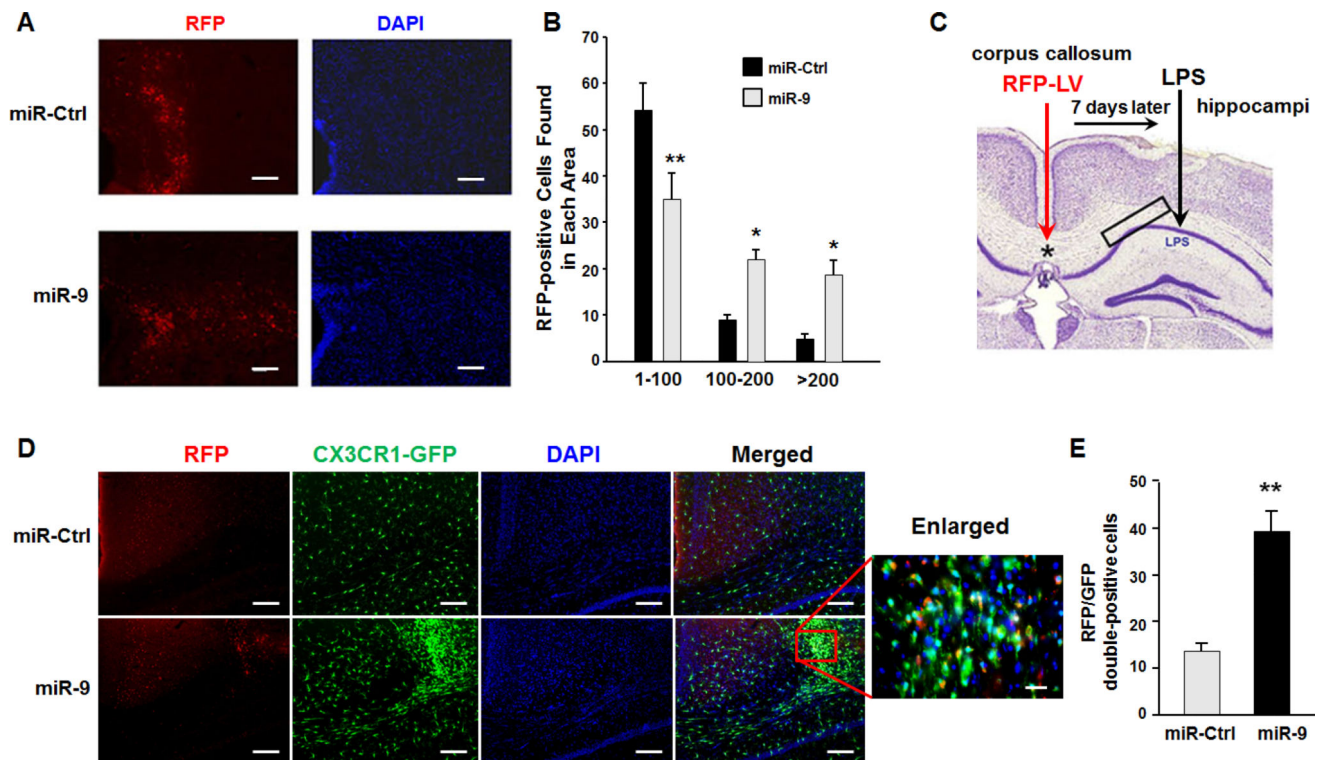
Figure 7. miR-9 promotes microglial migration in vivo

(A, B) miR-9 precursor-transduced microglia were transplanted into the striatum of mice followed by monitoring their migration in response to LPS. **(A)** Representative images of immunostaining for RFP-labeled cells *in vivo*. Microglia transfected with miR-control remained largely at the injection site while cells transfected with miR-9 migrated away from the injected sites toward the injury site. Scale bar=50μm. **(B)** Analysis of transplanted microglial migration in the striatum. Microglia in different sampling areas (0–100, 100–200, and >200μm away from the transplanted microglia) were counted in each mouse. **(C)** Schematic diagram showing *in vivo* locations of RFP-lentivirus (*) and LPS injection. **(D, E)** Transduction of microglia with miR-9 resulted in increased migration to the LPS-injected site compared with the miR-control group. **(D)** Representative RFP/GFP-positive microglia in the area (left panel). Scale bar=50μm. The area chosen for analysis of RFP/GFP positive microglial migration are shown. Scale bar=10μm. **(E)** Quantification of RFP/GFP-positive microglia in the specific area. N=5 animals/group. ** $p < 0.01$ vs miR-control group.